ELSEVIER

Journal of Power Sources 109 (2002) 347–355

JOURNAL OF POWER SOURCES

www.elsevier.com/locate/jpowsour

Creep behavior of Ni-12 wt.% Al anodes for molten carbonate fuel cells

Dongho Kim[a,*], Insung Lee[a], Heechun Lim[b], Dokyol Lee[a]

[a]*Division of Materials Science and Engineering, Korea University, 5-1 Anam-Dong, Sungbuk-Ku, Seoul 136-701, South Korea*
[b]*Korea Electric Power Research Institute, Korea Electric Power Corporation, 103-16 Moonji-Dong, Yusong-Ku, Taejon 305-380, South Korea*

Received 21 December 2001; accepted 12 February 2002

Abstract

Ni-12 wt.% Al anodes are fabricated for use in molten carbon fuel cells by tape casting and sintering. Sintering is performed in three steps, first at 1200 °C for 10 min in argon, then at 700 °C for 2.5 h in a partial oxidation atmosphere ($P_{H_2}/P_{H_2O} = 10^{-2}$), and finally at 950 °C for 5 min, 30 min or 1.5 h in hydrogen. Three anodes with different phases or microstructures are produced at different reduction times. One anode contains three phases, namely Ni–Al solid solution, Ni_3Al, and Al_2O_3. The amount of Al_2O_3 is extremely small at 5 min. A second anode also contains the three phases with the amount of Al_2O_3 comparable with that of Ni_3Al at 30 min. Third anode contains two phases, i.e. Ni–Al solid solution and Al_2O_3 formed at 1.5 h. The creep strains measured for the three anodes after a 100-h creep test are practically the same with an average value of 0.85%.

Keywords: Ni-12 wt.% Al anode; Molten carbonate fuel cell; Ni_3Al; Al_2O_3; Solid solution; Creep strain

1. Introduction

The operation temperature (923 K) of a molten carbonate fuel cell is higher than half the melting temperature of nickel and thus presents a very harsh thermal environment for a nickel anode. At such a high temperature, a metal will deform plastically over a period of time even when the applied stress is less than its yield strength as measured in a tensile test at that temperature [1]. This time-dependent deformation is called creep, and anode creep is still a main subject of MCFC research.

A great deal of research has gone into developing mechanisms for creep deformation. The mechanisms are now divided generally into four major groups [2], namely dislocation glide, dislocation creep, diffusion creep, and grain boundary sliding. Stress and temperature conditions dictate which of the four mechanisms predominates. The dependence can be easily visualized by a deformation mechanism map delineated in a stress-temperature space. Ashby [3] has made such a map for pure Ni. According to the map, dislocation creep or diffusion creep is the most predominant mechanism under the stress and temperature conditions of MCFC stacks. The dislocation creep involves dislocations moving along slip planes and overcoming obstacles by dislocation climb which requires diffusion of vacancies or interstitials. Thus, creep deformation is closely related to dislocation movement, and creep resistance can be achieved in principle by blockage of dislocations with obstacles, which is usually called 'strengthening'. Indeed almost all the attempts to enhance the anode creep resistance employ one of the strengthening mechanisms such as solute-, precipitation-, and oxide-dispersion-strengthening, or their combinations.

In our laboratory, efforts are continuing to be made to develop highly creep-resistant Ni–Al anodes. Initial efforts found [4] that, when sintered in a partial oxidation–reduction atmosphere, an Ni-5 wt.% Al anode showed the morphology of small Al_2O_3 particles dispersed in a network structure of the Ni–Al solid solution. The resulting high creep resistance is possibly due to a combination of solute- and oxide-dispersion-strengthening. The work has now been extended to an Ni-12 wt.% Al composition, in the expectation that an anode of this composition will have basically the same morphology as the Ni-5 wt.% Al anode but with an additional phase of Ni_3Al intermetallic compound and, accordingly, higher creep resistance due to extra precipitation strengthening. Three Ni-12 wt.% Al anodes have been fabricated with different phases or microstructures through

* Corresponding author. Tel.: +82-2-3290-3813; fax: +82-2-3290-3813.
E-mail address: hodong70@shinbiro.com (D. Kim).

0378-7753/02/$ – see front matter
PII: S0378-7753(02)00085-X

variation of sintering conditions, and the effect of these difference on creep behavior has been investigated.

2. Experimental procedure

The Ni-12 wt.% Al anodes were fabricated in a similar fashion to that for the Ni-5 wt.% Al anodes [4]. Elemental powders of Ni (carbonyl–nickel type 255, Inco) and Al (High Purity Chemicals) were used as starting materials and the green sheets were prepared by tape casting. Sintering of the green sheet was performed in three steps for Ni-12 wt.% Al anodes. First, the green sheet was heated at 1200 °C for 10 min in argon (99.9999% purity) atmosphere so that it could be turned into an equilibrium state of a two-phase mixture of Ni-5 wt.% Al solid solution and Ni_3Al, then at 700 °C for 2.5 h in a partial oxidation atmosphere ($P_{H_2}/P_{H_2O} = 10^{-2}$) so that small particles of Al_2O_3 could be formed in a dispersed state in the preexisting phases, and finally at 950 °C for 5 min, 30 min or 1.5 h in a hydrogen atmosphere so that NiO possibly formed at the stage of partial oxidation could be reduced back to Ni. The variation of reduction time was intentionally made for three designs of alloys with different phases or microstructures.

The phases of the anodes at each step of sintering were identified by means of X-ray diffraction analysis (XRD, Rigaku Geigerflex DMAX-II A). The microstructures were examined with field emission scanning electron microscopy (FE-SEM, Hitachi 6300) and Auger electron spectrometry (AES, Physical Electronics 680). A copper tube was used for the XRD experiments and the wavelengths of 1.5418 Å (Kα) and 1.5405 Å (Kα1) [5] were used for lattice parameter calculations. The creep test was performed in an apparatus shown in Fig. 1 at a temperature of 650 °C and a pressure of 100 psi for 100 h in hydrogen atmosphere. The creep specimens were fabricated with porosities at a similar level so that their creep strains, which are a sensitive function of porosity, could be compared directly with one another. The porosity of the creep specimen was measured using the Archimedes method (ASTM, C373-72).

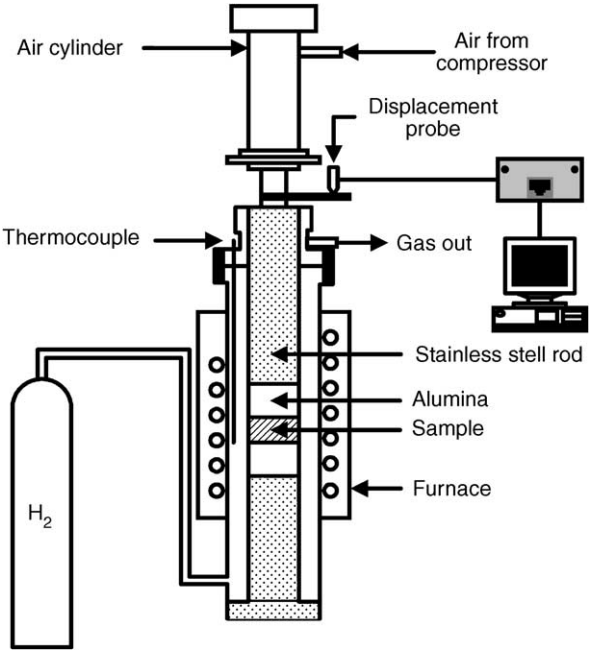

Fig. 1. Schematic diagram of apparatus used for creep tests [4].

3. Results and discussion

3.1. Phases

The XRD pattern for an Ni-12 wt.% Al specimen after sintering at 1200 °C for 10 min in argon atmosphere is shown in Fig. 2(a). It is found to represent a mixture of a simple cubic major phase (Cu_3Au structure) and a face-centred cubic minor phase with lattice parameters of 3.587 and 3.545 Å, respectively. The former phase was identified as Ni_3Al and the latter as the Ni-5 wt.% Al solid solution. The lattice parameter for Ni_3Al or Ni-5 wt.% Al solid solution is in excellent agreement with the respective value of 3.588 or 3.541 Å calculated from the XRD pattern of a specimen of the same phase fabricated similarly as the Ni-12 wt.% Al specimen from a mixture of Ni and Al powders with an appropriate composition, as will be mentioned later. It is interesting to note, however, that the lattice parameter for Ni_3Al deviates a little from the JCPDS value of 3.572 Å [6].

According to the phase diagram for the Ni–Al system [7], the above specimen is supposed to contain Ni_3Al and Ni-5 wt.% Al solid solution phases with 84 and 16 wt.%, respectively, at equilibrium. The actual wt.% of the Ni_3Al phase was estimated to be 86 from a calibration curve obtained from quantitative analyses made on various powder mixtures of Ni_3Al and Ni-5 wt.% Al solid solution with different weight ratios. Thus, the specimen is indeed in an equilibrium state.

The XRD patterns of the specimen after partial oxidation at 700, 800 and 900 °C for 2.5 h are given in Fig. 2(b) to (c), respectively. The specimen still consists of Ni_3Al and Ni–Al solid solution phases and no oxide phase whatsoever can be detected in the patterns after oxidation. This does not necessarily mean that oxides have not been formed during the oxidation process. It is more likely, and this is confirmed below from AES analyses, that oxides are indeed present in the specimen but that the amount is too small to be detected by X-rays.

The peak positions for the solid solution or Ni_3Al phase are practically the same as those measured before oxidation regardless of the oxidation temperature. Therefore, the phases present in the specimen before and after oxidation are deemed to be the same. The peak intensities, however, are affected by the oxidation and are dependent on the oxidation temperature. The peaks for the solid solution become stronger. In other words, the amount of the solid

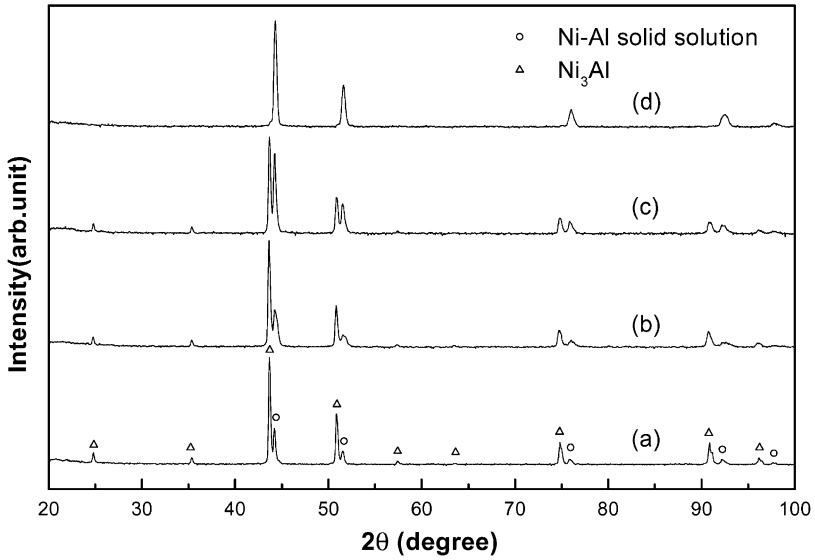

Fig. 2. XRD patterns for Ni-12 wt.% Al specimen (a) sintered at 1200 °C for 10 min in Ar and for specimens obtained after partial oxidation at (b) 700 °C; (c) 800 °C; and (d) 900 °C for 2.5 h.

solution increases as the temperature increases. On the other hand, the peaks for Ni_3Al remain almost constant until they suddenly become very weak at 900 °C. Thus, the oxidation has changed the relative amounts of the two phases, not the phases themselves, and the ratio of the amount of the solid solution to that of Ni_3Al increases with increasing temperature. As will be discussed later, the reduction process also decreases the amount of Ni_3Al. Therefore, in the following experiments, the partial oxidation temperature is set at 700 °C where the amount of Ni_3Al is still so large that some of the phase may remain in the specimen even after reduction.

The XRD patterns for the specimen reduced at 950 °C for various times after partial oxidation at 700 °C for 2.5 h are presented in Fig. 3. Comparison with the pattern given in Fig. 2(b) confirms the statement made above that the reduction process decreases the amount of Ni_3Al. Rather, it appears to induce the formation of a new phase of Al_2O_3. It is difficult, however, to detect the presence of the Al_2O_3 phase because most of the visible peaks for Al_2O_3, for example those at $2\theta = 35.2$, 43.4 and 57.6°, almost coincide those for Ni_3Al, as can be seen in Fig. 3(b). The exception is the peak at $2\theta = 24.7°$ which is sufficiently separated to be distinguished from that for Ni_3Al at 25.6°. Therefore, this peak could be used most conveniently for identification of the Al_2O_3 phase, but with appropriate magnification for a clear view. When the magnified view is presented so as to include also the peak for Ni_3Al at 25.6°, it alone can indicate whether the specimen contains either or both of the Al_2O_3 and Ni_3Al phases, though the Ni_3Al phase can be identified

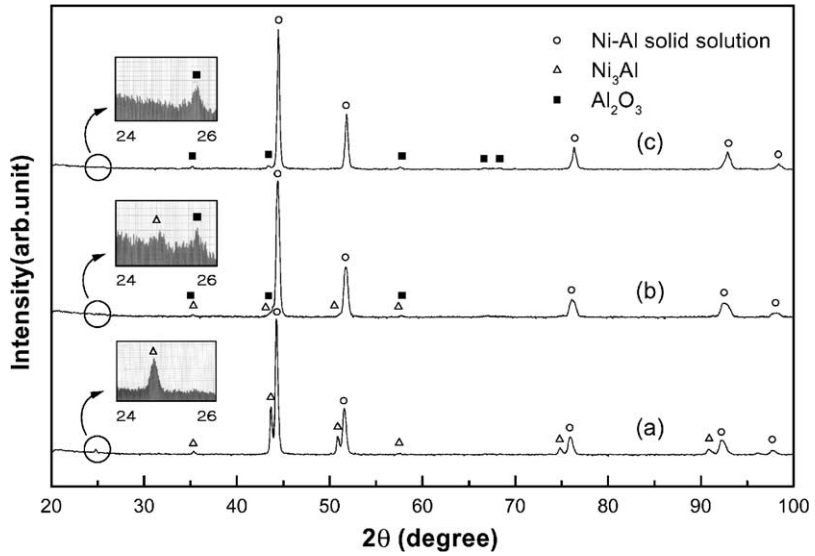

Fig. 3. XRD patterns for Ni-12 wt.% Al specimen obtained after reduction for (a) 5 min; (b) 30 min; and (c) 1.5 h.

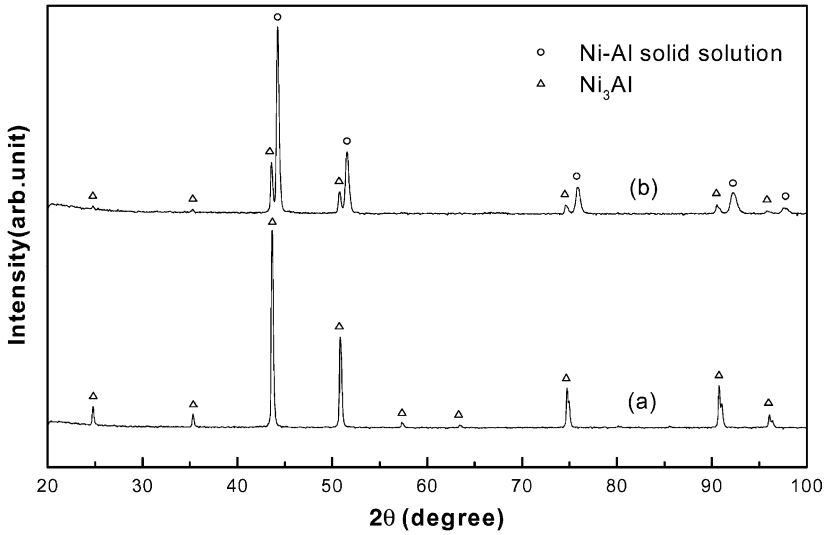

Fig. 4. XRD patterns for Ni-13.3 wt.% Al specimen: (a) sintered at 1200 °C for 10 min in Ar; and (b) after reduction for 30 min.

more easily by its intense peaks at $2\theta = 50.7$, 75.1 or 91.3° than by that at 25.6°. Such magnified views are shown in the insets of Fig. 3 and it can be clearly seen that Ni_3Al, both Ni_3Al and Al_2O_3, or Al_2O_3 are present in the specimen together with a major phase of Ni–Al solid solution at a reduction time of 5, 30 min or 1.5 h, respectively.

The reduction not only decreases the amount of Ni_3Al and induces the formation of the Al_2O_3 phase, but also alters the lattice parameter of the solid solution phase. It has been changed to 3.537 Å at a reduction time of 30 min and to 3.523 Å at 1 5 h though no practical change is noticed at 5 min. The Vegard law [5] allows an approximate prediction of the Al contents of the solid solutions from the values of the correspondings. The values are 5 wt.% at 5 min, 2.5 wt.% at 30 min and almost 0 at 1.5 h.

In order to understand the phase changes which occur in the Ni-12 wt.% Al specimen during sintering, a study was conducted on the oxidation behavior of each of the two phases present in the specimens. For this purpose, a specimen of Ni_3Al or Ni-5 wt.% Al solid solution was made from a mixture of the two elemental powders, with respective Al contents of 13.3 or 5 wt.%, through a routine of tape casting and sintering at l200 °C for 10 min in argon, i.e. using the same procedure as for the Ni-12 wt.% Al specimen shown in Fig. 2(a). The specimen was then sintered at 700 °C for 2.5 h in an atmosphere of $P_{H_2}/P_{H_2O} = 10^{-2}$, and at 950 °C for 30 min in hydrogen. This sintering schedule is exactly the same as that adopted for the Ni-12 wt.% Al specimen shown in Fig. 3(b).

The XRD patterns for the Ni-13.3 wt.% Al specimen before and after the additional sintering are given in

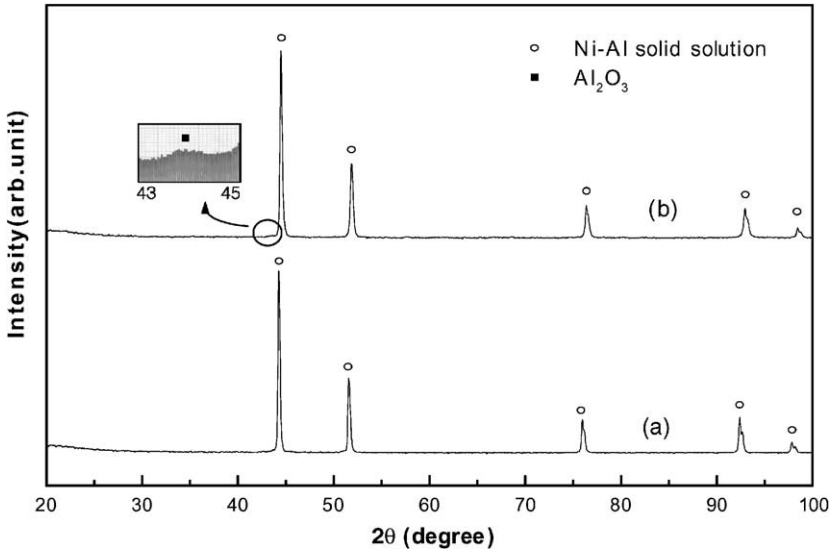

Fig. 5. XRD patterns for Ni-5 wt.% Al specimen: (a) sintered at 1200 °C for 10 min in Ar; and (b) after reduction for 30 min.

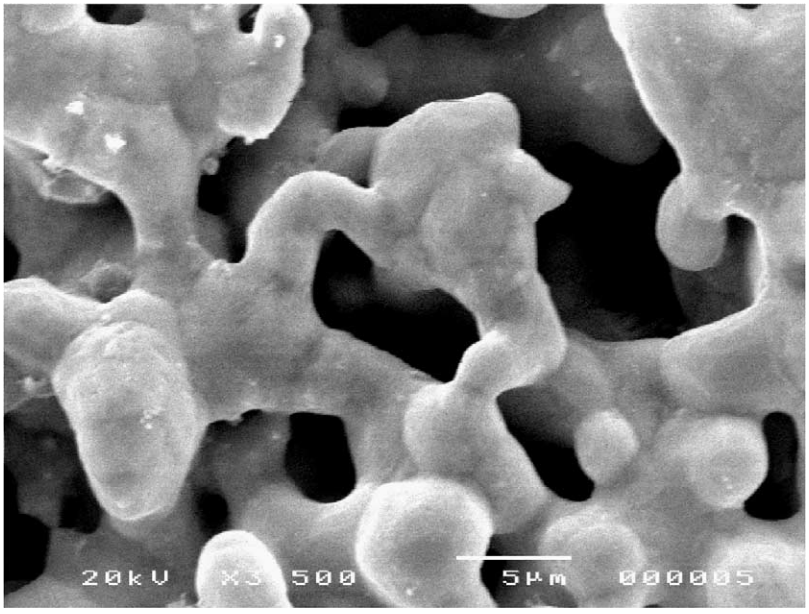

Fig. 6. Electron micrograph of Ni-12 wt.% Al specimen sintered at 1200 °C for 10 m in Ar.

Fig. 4. A single phase of Ni_3Al is present in the specimen before the additional sintering, but a considerable portion of the Ni_3Al phase has transformed to Ni–Al solid solution during additional sintering. The latter is probably due to the fact that aluminum atoms diffuse from the inside of each Ni_3Al grain to the surface to form aluminum oxide and leave behind a solid solution phase. Ironically, no aluminum oxide phase is detected in the XRD pattern after additional sintering, again possibly because the amount is extremely small. The composition of the newly formed solid solution is estimated to be Ni-5 wt.% Al from the measured lattice parameter value of 3.545 Å. Thus, the data in Fig. 4 have provided an explanation for the change in the relative amounts of Ni_3Al and solid solution phases during partial oxidation and reduction.

The XRD patterns for the Ni-5 wt.% Al specimen are presented in Fig. 5. Before the additional sintering, this specimen consists of a single phase of solid solution. A very small amount of Al_2O_3 exists together with the solid solution in the specimen after additional sintering, as can be detected from the data in the inset of Fig. 5. The peaks for the solid solution shift to the higher angle side after the additional sintering. This peak shift corresponds to a change in parameter from 3.541 to 3.535 Å, which implies that the

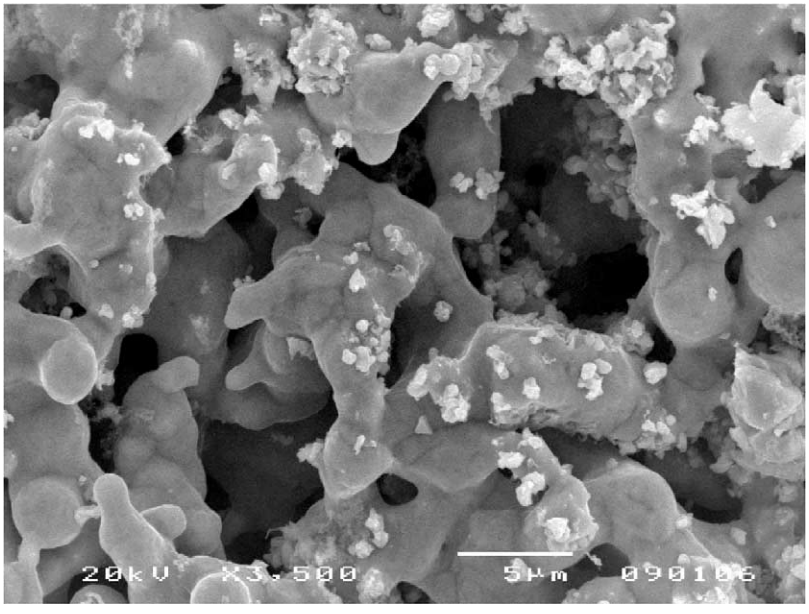

Fig. 7. Electron micrograph of Ni-12 wt.% Al specimen obtained after partial oxidation at 700 °C for 2.5 h.

aluminum content in the solution is less after the additional sintering. This can be justified in a similar manner as for Ni_3Al, and thus aluminum atoms diffuse from inside of each grain of the Ni-5 wt.% Al solid solution to the surface to form Al_2O_3, leaving behind a relatively Al-poor solid solution phase. Therefore, explanations for the change in lattice parameter of the solid solution and the formation of the Al_2O_3 phase during reduction are provided by the XRD data shown in Fig. 5.

3.2. Morphologies

A SEM of an Ni-12 wt.%A1 specimen sintered at 1200 °C for 10 min in argon is shown in Fig. 6; the corresponding XRD pattern is given in Fig. 2(a). The specimen has a typical network structure of the type usually seen in conventional anodes fabricated from pure nickel or nickel alloys by tape casting. When this specimen is partially oxidized at 700 °C for 2.5 h, numerous small particles are formed on the surface of the network structure, as shown in Fig. 7. According to AES in-depth analyses, the particles consist of nickel oxide, whereas, the matrix is covered with an extremely thin film of aluminum oxide. Thus, oxides of nickel and aluminum are indeed present in the specimen, but in amounts, too small to be identified in the XRD pattern in Fig. 2(b).

SEM of specimens reduced at 950 °C for various times after partial oxidation at 700 °C for 2.5 h are presented in Fig. 8. The structures are similar to that formed after partial oxidation, i.e. numerous small particles on the surface of a network structure. The number of particles increases with increasing time. Typical AES depth profile after reduction are shown in Fig. 9; the data are for a specimen reduced for 30 min. For a zone on the surface of the network structure with a particle, the outer region consists of metallic nickel whereas the inner region consists of aluminum oxide as can be seen in the profile (a). Metallic nickel must have been produced from NiO as a result of reduction that as mentioned above, exists in this zone after partial oxidation. According to profile Fig. 9(b), a zone without a particle is covered with a layer of aluminum oxide. This situation is explained schematically in Fig. 10, the diagram is an adaption of that reported by Haerig and Hofmann [8]. Before oxidation, the surface of the network structure is covered with native oxide of Al_2O_3. In the oxidizing atmosphere, nickel atoms diffuse from inside of the network structure to the surface, through such channels as grain boundaries or similar growth defects in the Al_2O_3 layer, to form NiO which will be reduced later to metallic nickel in the reducing atmosphere. Simultaneously, oxygen is transported along NiO/Al_2O_3 phase boundaries to the inside where it reacts with aluminum atoms to form aluminum oxide. The particles are therefore considered to be Al_2O_3 dispersions with their surfaces covered with metallic Ni.

In summary, three Ni-12 wt.% Al anodes have been prepared with different phases or microstructures. One anode contains three phases of an Ni–Al solid solution, Ni_3Al, and Al_2O_3 with the amount of Al_2O_3 extremely small at reduction

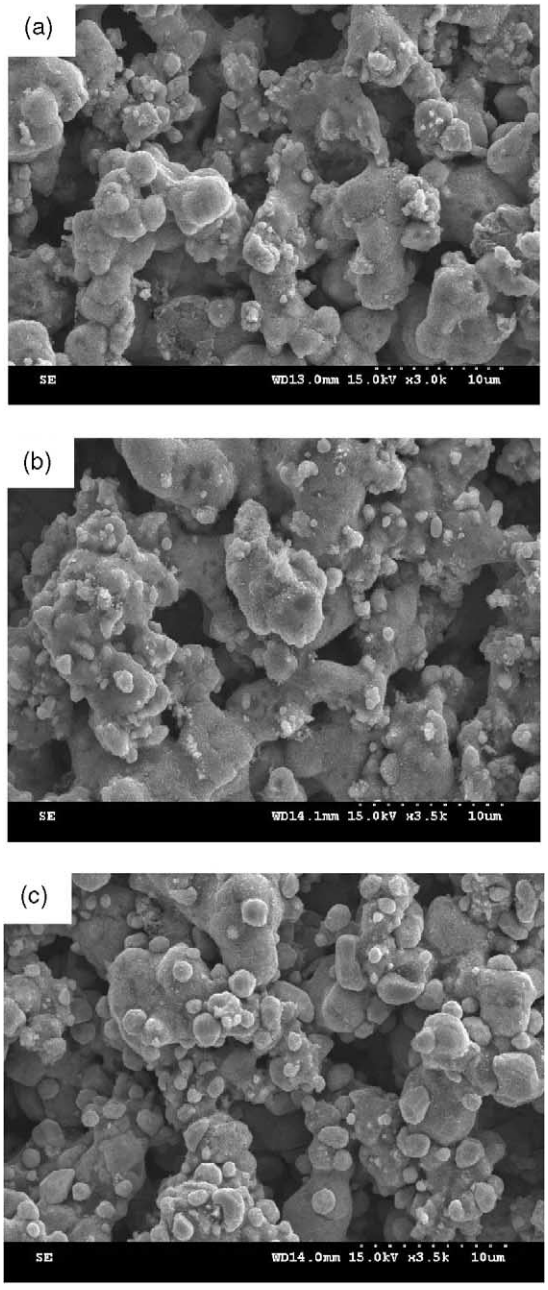

Fig. 8. Electron micrograph of Ni-12 wt.% Al specimen obtained after reduction for (a) 5 min; (b) 30 min; and (c) 1.5 h.

time of 5 min. A second anode also contains the three phases with the amount of Al_2O_3 comparable with that of Ni_3Al at 30 min. The third anode contains two phases namely a solid solution and Al_2O_3 formed at 1.5 h. As mentioned earlier, these three anodes were intentionally designed so that the effect of Ni_3Al, Al_2O_3, or their combination on the creep behavior of the Ni-12 wt.% Al anodecould be examined.

3.3. Creep behavior

The creep behavior of three Ni-12 wt.% Al anodes reduced for 5, 30 min and 1.5 h was investigated. For

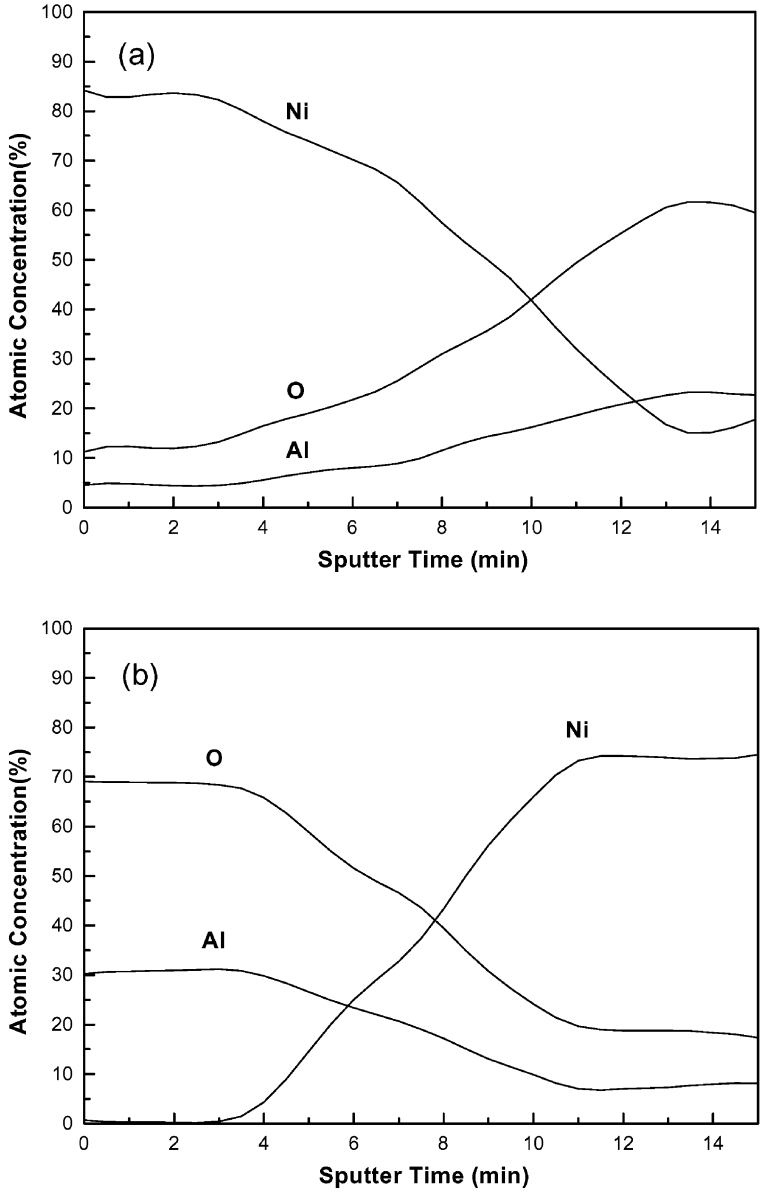

Fig. 9. AES depth profiles of Ni-12 wt.% Al specimen obtained after reduction for 30 min for the spots on surface of network structure (a) with; and (b) without a particle.

simplicity, these anodes will be referred hereafter to A, B and C (XCD patterns (a–c) in Fig. 3). As already mentioned in Section 2, the anodes were fabricated with porosities of a similar level for direct comparison of their creep strains, and the actual values of porosity were 55.2, 55.3 and 55.7% for anodes A, B and C, respectively. A creep curve obtained for anode C is shown in Fig. 11, those for anodes B and C are very similar. Also, the creep strains have been estimated from the specimen thickness before and after a creep test carried out for 100 h and they are 0.85, 0.76 and 0.93%, respectively, for anodes A, B and C. These values are actually very low and can be compared with the lowest one (2.3%), we obtained previously for Ni-5 wt.% Al anodes [4]. In the comparison, however, it has to be remembered that the Ni-5 wt.% Al specimen is a little more porous than the Ni-12 wt %Al specimen.

Anode B shows the smallest creep strain among the three specimens. When the experimental error bars are taken into account as in Fig. 12, however, the values of creep strain are considered to be practically the same for the three anodes with the average of 0.85%. As mentioned before, anode A, though analyzed by X-rays to contain only the two phases of Ni-5 wt.%A1 solid solution and Ni_3Al, was revealed later by AES analyses to contain also a very small amount of Al_2O_3 (some of which is in partial form), and, therefore, has all three sources of solute-, precipitation- and oxide-dispersion-strengthening. The amount of Ni_3Al is greatest in anode A. Anode B also contains the three phases, but the amount of

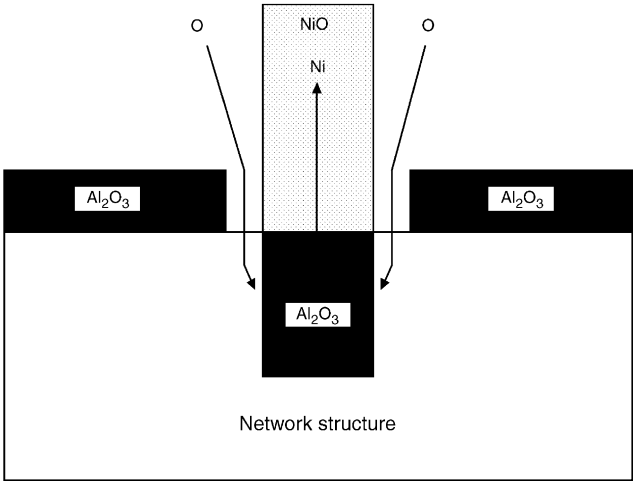

Fig. 10. Schematic diagram of Ni-12 wt.% Al specimen in oxidizing atmosphere, adapted from diagram suggested by Haerig and Hofmann [8].

Al_2O_3 is comparable with that of Ni_3Al and the aluminum content of the solid solution is less than that in anode A. Anode C contains two phases of a solid solution and Al_2O_3, but the so-called 'solid solution' is no more than pure nickel in consideration of its aluminum content. Therefore, the capacity for solute- or precipitation-strengthening is considered to be greatest in anode A, though the capacity for oxide dispersion strengthening is smallest. On the other hand, anode C is expected to show the greatest capacity for oxide dispersion strengthening and almost no capacity for solute- or precipitation- strengthening. Anode B is between anodes A and C in terms of the capacity for any of the solute-, precipitation- and oxide-dispersion-strengthening. Hence, it may be summarized that the capacities of solute-, precipitation- and oxide-dispersion- strengthening in each alloy add up to a similar level of total strengthening for the three anodes.

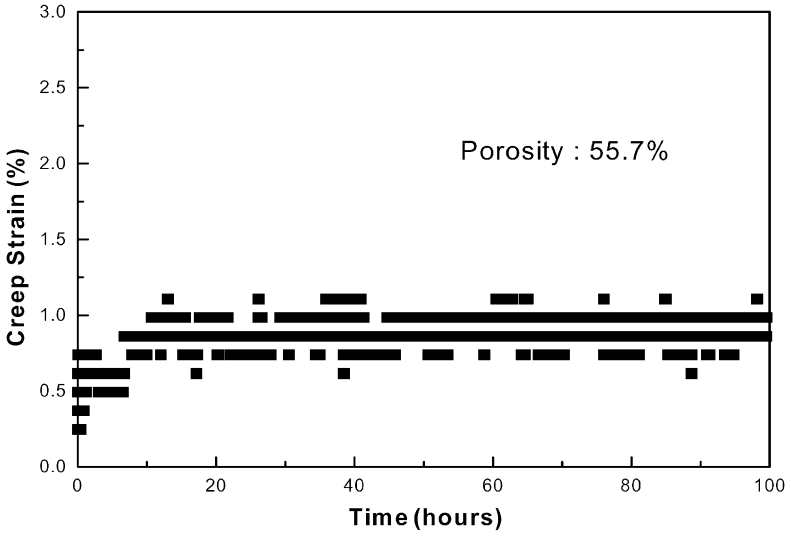

Fig. 11. Creep curve of Ni-12 wt.% Al specimen obtained after reduction for 1.5 h.

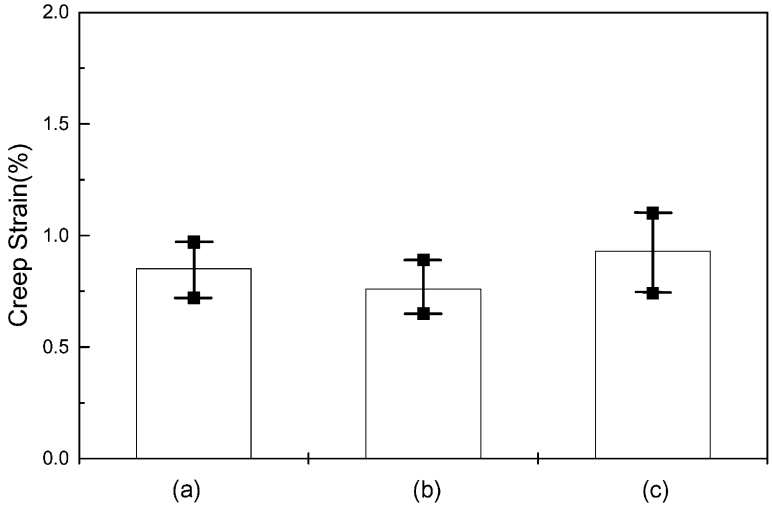

Fig. 12. Creep strains of an Ni-12 wt.% Al specimen reduced for (a) 5 min; (b) 30 min; and (c) 1.5 h.

4. Conclusions

Ni-12 wt.% Al anodes are fabricated for use in molten carbonate fuel cells by tape casting and sintering. Sintering is performed in three steps: (i) at 1200 °C for 10 min in argon; (ii) 700 °C for 2.5 h in a partial oxidation atmosphere ($P_{H_2}/P_{H_2} = 10^{-2}$); (iii) at 950 °C for 5, 30 min and 1.5 h in hydrogen. The creep behavior of the anodes is investigated with respect to their phases or microstructures and the following conclusions are made.

1. The anode is in an equilibrium state of a two-phase mixture of Ni-5 wt.% Al solid solution and Ni_3Al after sintering at 1200 °C for 10 min in argon atmosphere.
2. Partial oxidation increases the ratio of the amount of solid solution to that of Ni_3Al, reduction. Reduction also decrease the aluminum content in the solid solution or induces the formation of Al_2O_3 and to a greater extent as the reduction time is increased.
3. After reduction, the anode has a network structure with numerous small particles on its surface. The particles are dispersions Al_2O_3 with surfaces covered with metallic nickel. The number of the particles increases with increasing reduction time.
4. Three anodes with different phases or microstructures have been produced at different reduction times and respectively, comprise the following: (i) Ni_3Al, and Al_2O_3 with the amount of Al_2O_3 extremely small at 5 min; (ii) three phases with the amount of Al_2O_3 comparable with that of Ni_3Al at 30 min; (iii) two phases of solid solution and Al_2O_3 formed at 1.5 h.
5. The creep strains measured for the three anodes after a 100-h creep test are practically the same with an average value of 0.85%.

Acknowledgements

This study was financially supported by The Korea Electric Power Corporation and by The Korea Ministry of Commerce, Industry and Energy.

References

[1] C.R. Barrett, W.D. Nix, A.S. Tetelman, The Principles of Engineering Materials, Prentice-Hall, Englewood Cliffs, NJ, 1973, p.215.
[2] G.E. Dieter, Mechanical Metallurgy, 3rd Edition, McGraw-Hill, New York, 1986 (Chapter 13).
[3] M.F. Ashby, Acta Met. 20 (1972) 887.
[4] G. Kim, Y. Moon, D. Lee, J. Power Sources 104 (2002) 181–189.
[5] B.D. Cullity, Elements of X-ray Diffraction, 2nd Edition, Addison-Wesley, Reading, MA, 1978.
[6] JCPDS card 09-0097.
[7] B.A. Brandes, G.B. Brook (Eds.), Smithells Metals Reference Book, 7th Edition, Butterworth, Oxford, 1992, pp. 11–44.
[8] M. Haerig, S. Hofmann, Appl. Surf. Sci. 125 (1998) 99.